

Challenges in Simulating Pollutant Behavior in Watercourses with Diverse Ecological and Structural Features

W. Sobieski[†]

University of Warmia and Mazury in Olsztyn, Olsztyn, 10-900, Poland

[†] Email: wojciech.sobieski@uwm.edu.pl

ABSTRACT

The article presents the results of simulation studies conducted on a hypothetical watercourse with two simultaneous sources of pollutants of differing types, aimed at better understanding pollutant dispersion in complex riverine environments. The modeled watercourse incorporates a range of structural and natural elements, including a narrow riverbed section, a floodplain with vegetated zones, technical infrastructure (such as bridge supports and a side channel outlet), and various topographical features. The study was conducted using the Finite Volume Method within the ANSYS Fluent computational framework, integrating the Volume of Fluid model (Open Channel version), Species Model (for liquid pollutants), Porous Media Model (to represent vegetated zones), and Discrete Phase Model (for solid particles) into a unified simulation. In last part, a proposal for pollutant management strategies in selected water systems, where the risk of emergency situations is particularly high, is discussed. The primary objective was to identify challenging aspects of pollutant dispersion modeling in order to refine future research directions and methodologies.

Article History

Received November 18, 2024

Revised March 17, 2025

Accepted March 26, 2025

Available online June 3, 2025

Keywords:

Computational fluid dynamics simulation

Environmental engineering

Porous media

Conservative modeling

Aquatic systems

Pollutant transport

Numerical analysis

1. INTRODUCTION

Research on the impact of pollutants on the natural environment, particularly the mitigation of this impact, is a crucial aspect of modern science and engineering. Typically, considerations involve air, soil, and surface or groundwater pollution. In more advanced analyses, two or three groups of pollutants are taken into account simultaneously, such as settling dust on the soil surface penetrating into the soil and groundwater. In a broad sense, two main streams of environmental pollution research can be distinguished: predictive research (Ma et al., 2019; Xue et al., 2024) and design research (Chu et al., 2011; Veli et al., 2021; Li et al., 2024). In the first group, one can identify studies on the propagation of pollutants in the environment, the impact of these pollutants on the environment, and the duration of the harmful factors' influence. Predictive models often rely on historical data and are more accurate the more comprehensive the data is. In the second group, efforts are focused on finding solutions to eliminate or reduce pollution sources (design of waste disposal sites, post-production heaps, filters, containers, etc.), limiting the spread of pollutants (design of channel systems, drainage ditches, hydraulic infrastructure, etc.), as well as various solutions related to

environmental remediation. Regardless of the approach, research can address continuous interactions, exemplified by municipal or industrial wastewater issues, or singular events resulting from accidents and disasters.

In the context of modeling, two main types of models are distinguished: statistical models (including those using random algorithms or artificial intelligence) (Korotenko et al., 2004; Montazeri et al., 2023; Poursaeid, 2023) and conservative models (Lee et al., 2013; Zheng et al., 2016; Alvir et al., 2022; Hadžiabdić et al., 2022). Statistical models take into account population density, degree of industrialization, agricultural intensity, geological and hydrological conditions, among others. Conservative models are based on the physics of phenomena and processes such as advection, convection, diffusion, dispersion, and others. If the modeling of pollutant propagation is to be based on the physics of phenomena, a crucial aspect is identifying the type of mixtures to occur in the planned model and selecting the appropriate mathematical apparatus. Conservative models can be analytical or numerical, requiring the use of simulation techniques, with the model's complexity and the number of spatial dimensions varying significantly. The scale of the model plays a key role here, with a simplification distinguishing micro, meso, and macro scales. The

microscale involves modeling pollutant spread in very small areas, on the order of tens or at most hundreds of meters, for example, at the confluence of watercourses or in selected elements of hydraulic infrastructure. The mesoscale relates to modeling pollutant spread over areas on the order of kilometers, such as along a river or in a small water reservoir. The macroscale concerns modeling pollutant spread over areas on the order of tens or hundreds of kilometers, for example, along entire river basins or in large water bodies. An example of microscale analysis could be the modeling of the propagation of oil-derived pollutants due to a pipeline rupture crossing a river channel, as described in reference (Agranat et al., 2021). A 3D model was applied, covering a domain with dimensions of $6 \times 4 \times 2$ [m]. An example of mesoscale analysis can be found in reference (Diener, 2019), where the author investigated pollutant propagation in Lake Rådasjön. A 3D model was used, and the lake's surface area was approximately 2 [km²]. On the other hand, an example of macro-scale research can be found in article (Zima, 2019), where the area of interest was Puck Bay, with an area of about 364 [km²].

An aspect strongly related to the model scale is the assumption regarding the number of dimensions in the simulation model. In this context, models are distinguished as 1D, 2D, 2.5D, and 3D. 1D models describe the spread of pollutants in one dimension, most commonly along the river or stream channel (or a network of rivers and streams), usually based on mass balance equations. They are useful for simple cases and have an approximate application. 2D models describe the spread of pollutants in two dimensions, often along the course of a waterway and in the transverse direction. These models typically rely on advection-diffusion or advection-dispersion equations. Incorporating these equations allows for a more realistic modeling of pollutant spread in space and time. 2.5D models describe the spread of pollutants in two dimensions but also take into account the local water depth, generally variable in time and space. Models in this category often rely on the Saint-Venant equation or shallow water equations. 3D models describe the spread of pollutants in three dimensions and most commonly use the Navier-Stokes equation. Currently, the most popular method for creating conservative models of flow systems in 3D space is the Finite Volume Method (FVM), which involves surface and volumetric balances of mass, momentum, and energy within a single finite volume.

The application of a simulation approach requires the development or availability of highly specialized software. Individual computer programs can be either universal or dedicated to specific applications or locations. In the review paper (Zieminska-Stolarska & Skrzypski, 2012), several specialized computational programs for modeling pollutant propagation in 1D, 2D, 2.5D, and 3D space were listed. It turns out that the use of full three-dimensional models in this field is still sporadic, mainly due to the immense computational power required to obtain solutions, especially when the scale of the study needs to be sufficiently large. Literary studies have also shown that typical, universal software, such as ANSYS Fluent or OpenFOAM, are exceptionally rarely used in the context of the discussed issues. This observation became

a motivation to undertake research and determine to what extent standard CFD (Computational Fluid Dynamics) tools can currently be useful in modeling the propagation of pollutants in watercourses. It was assumed here that the user would have access to relatively typical computer hardware, rather than high-performance computing clusters.

This article presents a pioneering numerical analysis of three-dimensional microscale water flow using advanced CFD tools. Rather than simulating a specific case, the developed model serves as a foundation for exploring pollutant dispersion in aquatic environments and aims to bridge knowledge gaps in three-dimensional conservative modeling. Targeted at environmental engineers and researchers in related fields, this work demonstrates the potential of CFD to address complex questions about pollutant behavior in water systems. Despite extensive experience in CFD, the author encountered unexpected challenges, particularly regarding the achievable spatial and temporal scale of such models. This prompted exploratory research using the ANSYS Fluent 2022R2 software, with detailed insights focusing on its unique capabilities. Notably, the study combines multiple models – Volume of Fluid, Species Model, Porous Media Model, and Discrete Phase Model – within a single, large-scale 3D simulation. To the author's knowledge, this is the first attempt to utilize this specific configuration of multiphase models in a single analysis, providing a fresh perspective on CFD's applicability to environmental sciences.

2. MATERIALS AND METHODS

2.1. Geometry of the Watercourse

Figure 1 depicts a model microscale watercourse, which serves as the subject of the research described in the article. As mentioned earlier, this watercourse does not represent any real-world system and was specifically prepared for the numerical test. It was assumed that the model should include elements such as: an area with a distinct, narrow riverbed (A); a floodplain area (B) containing a zone with aquatic vegetation (C); technical infrastructure elements (here, bridge supports and the outlet of a side channel); other features of the riverbed (here, stones or other undefined objects lying on the

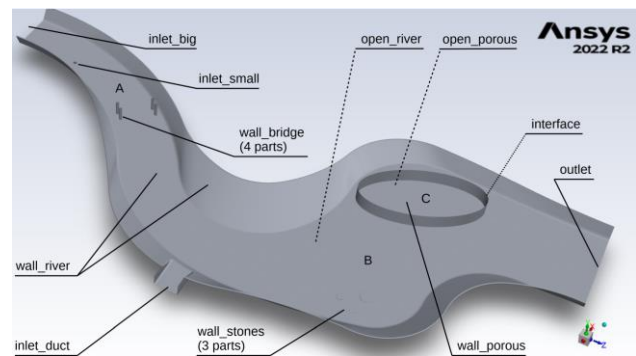


Fig. 1 Geometry of the model watercourse

bottom). The level of detail was significantly limited to avoid unnecessary grid densification, which would increase computational power requirements. For the purposes of the test, it was assumed that the shape of the water surface should be tracked during the inflow, and the liquid phase would consist of two components: so-called clean water flowing in the main stream and so-called dirty water, introduced into the watercourse through a side channel. A small additional inlet, representing the injection point of some solid particle pollutants (it could be a source of microplastics, for example (Bondelind et al., 2020)), was planned in the model. The type of pollutants in the dirty water and the nature of the solid particles are not specified due to the general nature of the numerical test. It is important to emphasize that such assumptions, especially those related to the media, result from knowledge of the mathematical apparatus, approaches to modeling multiphase systems, and the general capabilities of computational packages such as ANSYS Fluent or OpenFOAM.

After preparing the geometry of the watercourse, the entire computational domain was divided into two zones: the water zone (named “zone_river”) and the zone representing the area covered with aquatic vegetation (named “zone_porous”). The vegetation zone is connected to the river zone by two surfaces labeled “interface” on the diagram. These surfaces are two because both zones must form two independent geometric volumes in space.

The geometric model consists of the main clean water inlet (“inlet_big”), representing a selected cross-sectional surface of the watercourse, the auxiliary clean water inlet (“inlet_small”), representing the previously mentioned injection point of solid particle pollutants, the side inlet (“inlet_duct”), representing the inflow of dirty water, and the outlet (outlet). Additionally, the geometry includes the lower and side surface of the water zone (“wall_river”), the lower surface of the vegetation zone (“wall_porous”), and two auxiliary surfaces (“wall_bridge” and “wall_stones”). The first represents the bridge supports, and the second represents objects such as stones lying on the bottom of the floodplain, visible in the lower part of the watercourse. The geometry is closed by the upper surface of the river zone (“open_river”) and the upper surface of the vegetation zone (“open_porous”). These surfaces are not visible in Fig. 1 as they would obscure objects behind them.

The main inlet is located in the XY plane. The outlet is parallel to it, with a distance of 84.425 meters between them. The length of the riverbed, measured at the center of its flow, is just under 90 meters. The width of the river varies from 8 meters at the inlet to approximately 30 meters at the widest point of the floodplain. At the outlet, the width of the watercourse is 14 meters. The height of the domain is set at 2 meters, with the initial water surface located 0.9 meters above the bottom. The total area of the “open_river” and “open_porous” surfaces is 1627 [m²]. The area covered with vegetation has an elliptical shape with diameters of 17 and 8.2 meters. The positioning of the computational domain was chosen so that the point 0 on the Y-axis lies on the lower, flat, and horizontal surface

of the watercourse bed. This arrangement facilitates the later definition of boundary conditions.

2.2. The Finite Volume Method for multiphase flows

In the numerical investigations, the Finite Volume Method (FVM) is used, which involves two main types of balances: the surface balance and the volumetric balance. The surface balance describes the exchange of a certain quantity with the surroundings through the fluxes flowing through the surface of a Finite Volume. The volumetric balance describes the change of a certain value inside a Finite Volume. The main set of balance equations can be expressed as follows (Sobieski, 2011, 2013):

$$\left\{ \begin{array}{l} \frac{\partial \rho}{\partial t} + \text{div}(\rho \vec{v}) = 0 \\ \frac{\partial(\rho \vec{v})}{\partial t} + \text{div}(\rho \vec{v} \vec{v} + p \vec{I}) = \\ \text{div}(\vec{\tau}^l + \vec{\tau}^t) + \rho s_b \\ \frac{\partial(\rho e)}{\partial t} + \text{div}(\rho e \vec{v} + p \vec{I} \vec{v}) = \\ \text{div}[(\vec{\tau}^l + \vec{\tau}^t) \vec{v} + \vec{q}^l + \vec{q}^t] + \rho s_e \end{array} \right. \quad (1)$$

where: ρ – density [kg/m³], \vec{v} – velocity [m/s], p – static pressure [Pa], \vec{I} – unit tensor [-], $\vec{\tau}^l$ – viscous stress tensor [Pa], $\vec{\tau}^t$ – turbulent stress tensor [Pa], s_b – source of forces [N/m³], e – sum of kinetic and internal energy, \vec{q}^l – laminar heat flux [J/(m²·s)], \vec{q}^t – turbulent heat flux [J/(m²·s)], s_e – sources of heat [J/(m³·s)]. Note, that the set of balance (or transport) equations (1) is incomplete and requires additional “closure” models to describe individual problems (Sobieski, 2013). After performing the calculations, the system of equations (1) provides information about the distributions of arbitrary scalar and vector fields throughout the entire computational domain.

The system of equations (1) is valid for single-phase flow. In the case of multiphase flows, this system may still be applicable, but it needs to undergo appropriate modifications. Identifying the appropriate scenario (Fig. 2) is the first and crucial step in developing a numerical model. Any subsequent change in assumptions may necessitate changes to the mathematical apparatus, which practically means reconfiguring the entire model or its parts, sometimes requiring modifications to the geometry and regenerating the computational grid.

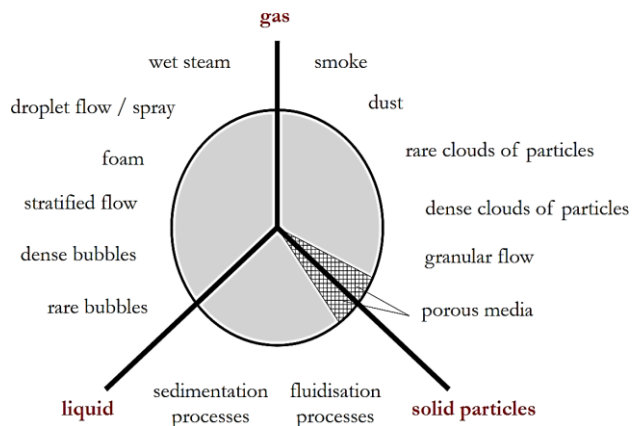


Fig. 2 Simplified visualization of possible types of liquid-gas-solid systems in a multiphase flow

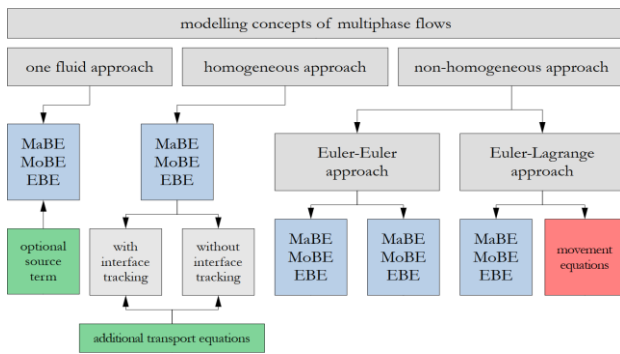


Fig. 3 Main modelling concepts of multiphase flows (Sobieski & Šarler 2023). (MaBE – Mass Balance Equation, MoBE – Momentum Balance Equation, EBE – Energy Balance Equation)

Experience shows that it is far more advantageous to create a numerical model from scratch than to modify an existing one. In the latter case, there is an increased risk of errors, misinterpretation of data by the software, or the presence of a non-obvious setting for one of the options. Such issues arose in the numerical test described, as will be discussed later in the article.

In the field of CFD, there are two main groups of models dedicated to multiphase flows (Fig. 3): homogeneous and heterogeneous. It is crucial to note that these models cannot generally be applied together (mainly due to computational costs), and one typically needs to decide on one of these options. This consideration applies to programs like ANSYS Fluent and OpenFOAM, and it is possible that some other software packages have achieved such a combination. In both homogeneous and heterogeneous models, interactions between components of the mixture are defined using additional closure sets, often referring to source terms in the balance equations. It is good practice to formulate the problem in such a way that the number of mixtures and components in them is as small as possible. An extreme example of this approach is the so-called single-fluid models.

The single-fluid approach can be used in two ways. In the first option, the system of equations (1) is solved, and based on the obtained data, the possibility of a particular phenomenon occurring is estimated. An example could be assessing the potential occurrence of cavitation based on the pressure field obtained from the simulation. In the second option, the system of equations (1) is supplemented with appropriate closures of source terms. Examples include the Porous Media Model (PMM) or Porous Jump Model (PJM), where source term in the momentum equation introduces additional resistance, simulating the presence of a porous medium. In this approach, the focus is not on modeling the medium itself but rather on the effect of its existence. The mentioned models differ in that PMM is applied to selected volumes (the entire domain or specific zones), while PJM is applied to selected surfaces, simulating a sudden pressure jump caused by the presence of semi-permeable membranes, grids, meshes, perforated sheets, etc. The flow resistance effect posed by the porous medium is described by Darcy's, Forchheimer's, or similar equations. It is essential

that the volumes or surfaces to which PMM or PJM should be applied be clearly identified.

The homogeneous approach involves solving the system of equations (1) with the assumption that variables such as density, pressure, or velocity refer to the mixture as a whole. Mass or volume fractions of individual components are determined using additional balance equations, having the same structure as those visible in the system of equations (1). The number of additional equations is one less than the number of mixture components, as the mass or volume fractions of mixture components always sum to one. The homogeneous approach has various variants. The Mixture Model (MM) is commonly applied when there are no significant chemical reactions between the components. This model is typically used to describe flows with phase change, such as evaporation and condensation or cavitation phenomena. The number of mixture components in MM is usually small, which explains why this model is sometimes referred to as the Two-Fluid Model. The Species Model (SM) has a similar nature but is dedicated to modeling mixtures with (although not necessarily) chemical reactions, for example, in combustion processes. In such cases, the number of components can be relatively large. Another variant of the homogeneous approach is the Volume of Fluid (VoF) model. It is designed for modeling flows with a free surface or two immiscible fluids. In a general sense, both phases can be homogeneous mixtures, with possible phase changes or chemical reactions between them. A characteristic feature of the VoF model is algorithms that detect the position of the phase interface. The VoF model has a variant called Open Channel, used for modeling liquid flows in rivers, channels, water bodies, etc. Additional options allow the modeling of waves on the free surface of the liquid.

The nonhomogeneous approach involves each phase having its own set of conservation equations, leading to obtaining individual distributions of scalar and vector fields. Similar to the previous approach, interactions between phases are defined by appropriate closures, such as interphase mass, momentum, or energy exchange coefficients. It is crucial to note that there are two variants of nonhomogeneous models: Euler-Euler (referred to as the Eulerian Multiphase Model, EMM, in the literature) and Euler-Lagrangian. In Euler-Euler models, dispersed phases are not treated as collections of individual objects. During simulation, only the volume or mass fractions of individual mixture components are tracked. In Euler-Lagrangian models, the background phase (fluid in which the dispersed phase is located) is modeled according to the Eulerian description, while dispersed phases are described using the Lagrangian approach. This allows the observation of the location, trajectory, and behavior of individual objects, such as solid particles in the fluid, liquid droplets in a gas or another immiscible liquid, or gas bubbles in a liquid. Euler-Lagrangian models are relatively complex to configure and computationally expensive. In recent years, they are often created based on different numerical methods using various computer programs. This is done by combining Finite Volume Method (FVM) or Lattice Boltzmann Method (LBM) (Bhatnagar et al., 1954, Sukop & Thorne, 2006) with

Discrete Element Method (DEM) (Cundall & Strack, 1979), Smoothed Particle Hydrodynamics (SPH) (Liu & Liu, 2003), or other meshless methods. This type of approach is sometimes referred to as hybrid modeling (Zaidi, 2020). It's worth noting that in many cases, different mathematical models can be applied to model the same phenomena, making it challenging to choose a strategy to achieve the set goals. For example, cavitation phenomena can be modeled using MM or EMM. Another example is the modeling of fluidization phenomena: using EMM or a Euler-Lagrangian type model. In the latter case, calculations can be carried out by combining, for instance, OpenFOAM (FVM) or Palabos (LBM) or OpenLB (LBM) with the YADE program (DEM). Another model designed to describe systems consisting of a continuous phase with dispersed spherical solid particles, bubbles, or droplets of another liquid (treated as point masses) is the Discrete Phase Model (DPM). The dispersed phase must have a relatively small volume fraction (maximum 0.1) and can exchange mass, momentum, and energy with the continuous phase. DPM can be applied in two variants, with one-way or two-way interaction. In the first variant, it is assumed that the dispersed phase does not affect the behavior of the liquid phase, meaning that particle injection and trajectory calculations are performed after the main simulation based on the calculated velocity field. In the second variant, the consideration of mutual interactions is carried out again at each time step.

The above description of multiphase models is very general and does not fully showcase the potential of the available options. For example, in the implementation of the DPM in the ANSYS Fluent package (Ansys Fluent User's Guide, 2022), numerous additional physical phenomena can be considered. These include the influence of gravity and electromagnetic fields, thermophoresis, Brownian motion, the Saffman effect, the Magnus effect, virtual mass effect, various types of inter-particle collisions (raising the question of selecting a body model), changes in particle mass or size, and their coalescence or breakup. There are various boundary conditions for particles, such as particle passage through a wall without reaction, particle adhesion to walls, particle reflection off walls with or without damping, particle sliding on walls, or the formation of a particle film on walls. Another aspect is the optional modeling of the impact of wall roughness on particle behavior. Additional settings in the DPM model concern particle types (massless, inert, droplet, combusting, multicomponent), particle injection types (single, group, cone – only for 3D cases, surface, volume – only for non-DEM 3D cases with unsteady particle tracking), injector types (plain-orifice atomizer, pressure-swirl atomizer, air-blast-atomizer, flat-fan-atomizer, effervescent-atomizer, file, condensate), particle distribution methods (uniform, rosin-rammler, rosin-rammler-logarithmic, tabulated), definition of heat transfer coefficient (constant-HTC, Nusselt-number, Ranz-Marshall, Hughmark, Tomiyama), method of calculating drag coefficient (spherical, nonspherical, Stokes-Cunningham, high-Mach-number, Ishii-Zuber, Grace), and many other considerations. There is also a variant model called Dense Discrete Particle Model (DDPM), the use of which requires defining yet another

set of options. A similar multitude of options and variants exists for each of the aforementioned models, often making the modeling of multiphase systems a non-trivial task. This task becomes even more complicated when attempting to include multiple multiphase models in a single simulation. Not all of these models can be used together, and if they can, additional issues related to the order of defining individual model elements or their interaction may arise.

3. RESULTS AND DISCUSSION

3.1. Generation of the Numerical Mesh

The computational domain shown in Fig. 1 underwent spatial discretization using tetrahedral elements. Due to significant changes in the cross-sectional surface of the domain and the obstacles present, an attempt was not made to generate a typically more favorable “sweep” mesh. Such a mesh is typically used for slender and long geometries, such as pipelines or channels. It was assumed that in the general case, the geometry of the watercourse would be complex enough that “sweep” meshes would not be applicable. The basic size of a single mesh cell was set to 0.2 [m] throughout the domain. This value was reduced to 0.1 [m] on the walls of the bridge supports and on obstacles lying on the bottom. An inflation layer with a thickness equal to the basic size of a single mesh cell at a given location was added to all walls. After the initial mesh generation, it was found that the quality coefficients were very poor on the lateral edges of the upper surface, where the angle between the contacting planes was acute. To eliminate problematic areas, these edges were rounded with an arc of radius 0.2 [m]. This change should not significantly affect the course of the numerical test described in the article, especially since it concerns areas above the water level. After this modification, a mesh consisting of 6 005 729 cells was obtained (Fig. 4). The minimum orthogonality coefficient was 0.1, and the maximum skewness was 0.9. These indicators fall within an acceptable range. Subsequent calculations were stable, confirming that the developed numerical mesh is sufficiently accurate. A classical mesh independence study, which involves generating multiple meshes of varying densities and analyzing their impact on selected results, was not conducted. This decision was driven by the exploratory nature of the study, which focuses on the



Fig. 4 A view of the final numerical mesh

integration of multiple multiphase models within a single simulation. Additionally, computational resource limitations precluded the use of finer meshes than the one applied in this work.

The next step in the configuration was the selection of an appropriate and simultaneously executable set of mathematical models and closures. Firstly, a non-stationary type of analysis was chosen, and gravity was activated in the $-y$ direction. The Species Model (SM) was employed to describe the mixture of clear water and dirty water. It was assumed that clear water (“water-clear”) had a temperature of 10 [°C], with a density and dynamic viscosity of 999.7 [kg/m³] and 0.001306 [Pa·s], respectively. As the second liquid phase, water (“water-dirty”) was also selected, but with a temperature of 15 [°C], density of 999.1 [kg/m³], and viscosity of 0.0011375 [Pa·s]. The parameters were determined using the OMNI Calculator software (Omni Calculator, 2024). For the purposes of the test, no specific contaminants were considered. It was assumed that the so-called “water-dirty” constitutes a single medium with averaged parameters. The mixture of clear water (first component of the mixture) and dirty water (second component of the mixture) was named “water-mixture”.

During the analysis of a specific case, there may be a need to consider changes in the parameters of mixture components over time at selected or all inlets to the computational domain. In the approach applied in the article, this is possible indirectly by changing the values of averaged material parameters. In the ANSYS Fluent software, functions for changing the material parameters over time can be defined using the Named Expression tool or through User Defined Functions. Technically, this is not difficult but requires the development of appropriate functions based on additional analytical models, historical data, or other methods. It is worth noting that any division of the liquid phase into multiple components is also relatively easy to implement, as it does not require changes to the adopted mathematical apparatus. It would be sufficient to define more materials and then change the composition of the corresponding mixtures. Similar changes would need to be made if there is a need to consider additional components in the gas phase. The gas phase would then be composed of a mixture, defined in the same way as the water mixture described above.

The next step in configuring the simulation model was to activate the Volume of Fluid (VoF) model. As mentioned earlier, this model is used, among other things, for simulating flows with a free surface, in this case, a system consisting of air and a liquid mixture of two components. In the VoF model (at least in the variant implemented in the ANSYS Fluent software), the order of components is important, as the first phase must be the gas phase (here: “air”), and the second phase must be the liquid phase (here: “water-mixture”). Due to the nature of the flow, the Open Channel variant of the VoF model was used to simulate the assumed flow. This variant is specially adapted for open flow systems. To ensure greater stability in the calculations, the “Implicit Body Force” option was also enabled, changing the default method of introducing body forces into the model. The surface

tension at the interface of the two phases was assumed to be constant and equal to 0.072 [N/m].

In the analyses of flow dynamics, only the mass balance equation and the momentum balance equation are used. In the case of the Species Model (SM), the energy equation must always be activated. In the described model, the properties of the mixture of pure water and dirty water were first defined, providing only their density and viscosity. Then, the SM was activated, resulting in the extension of the required set of material data. In such cases, the new parameters include specific heat, thermal conductivity, molecular weight, standard state enthalpy, and reference temperature. Due to the test nature of the model, default parameters proposed by the program were used in the simulation. In situations where thermal analysis would be of particular importance, these parameters would need to be more precisely defined, either by introducing averaged values for the considered temperature range or by using appropriate approximation functions.

3.2. Configuration of the Porous Media Model

Another element in creating the simulation model was the development of a method to account for the vegetation in the selected flow zone. Considering individual plants, their stems, or leaves is unrealistic due to the difficulties in obtaining relevant data and the unimaginable size of the computational grid. It seems that this task exceeds the capabilities of even the most efficient computing clusters. The second issue is the justification of such an approach. In the model described here, it was assumed from the outset that the vegetated area would be treated as a porous zone, where the Porous Media Model (PMM) would be activated. This explains why the geometry was prepared in such a way at the very beginning to obtain two zones in one computational domain. If this had not been done, the subsequent configuration of PMM would be impossible for selected areas of the domain.

In ANSYS Fluent, the hydrodynamic parameters of the porous medium are defined using the three-dimensional version of the Forchheimer equation (if the coefficient $\beta = 0$, the equation reduces to Darcy's law) (Ansys Fluent User's Guide, 2022)

$$s_i = - \left(\sum_{j=1}^3 D_{ij} \mu v_j + \sum_{j=1}^3 C_{ij} \frac{\rho |v| v_j}{2} \right) \quad (2)$$

and

$$D_{ij} = \begin{bmatrix} \frac{1}{k} & 0 & 0 \\ 0 & \frac{1}{k} & 0 \\ 0 & 0 & \frac{1}{k} \end{bmatrix}, \quad (3)$$

$$C_{ij} = \begin{bmatrix} 2\beta & 0 & 0 \\ 0 & 2\beta & 0 \\ 0 & 0 & 2\beta \end{bmatrix}, \quad (4)$$

where: k – permeability [m²], β – Forchheimer coefficient [1/m].

Even though the mathematical expression is straightforward, estimating the values of the coefficients k and β can be challenging. Since no helpful literature was

found, the model assumed that Darcy's law would apply to the flow ($\beta=0$) with $1/k=11809949$ (it is worth noting that the discussion regarding the applicability ranges of Darcy's law and Forchheimer's law is still ongoing, as exemplified by the study of Arthur (2018)). The permeability value was estimated based on earlier experimental studies on the pressure drop of water in a filtration column filled with glass beads (Sobieski et al.). Three bead diameters were considered: 4, 6, and 8 [mm], with larger diameters resulting in smaller flow resistances. Here, 1/4 of the average value obtained for 8 [mm] beads was adopted. This estimation method is imperfect but allowed for the observation of a significant impact of the porous zone on the simulation. Additionally, taking some reference value protected against providing excessively large values. The problem of determining the coefficients in the Forchheimer equation is well-known in the literature. Previous studies by the author on water flow through sands and gravels showed that the use of available empirical formulas can yield permeability values differing by several orders of magnitude. Since determining this coefficient's value is challenging for typical flows, it becomes even more difficult in non-standard cases. An additional complication is that aquatic vegetation, in general, can exhibit a tremendous variety of forms and structures, fundamentally filling the space in an anisotropic manner. Anisotropy can be accounted for in the model, as evident in equations (3) and (4). To define the porous zone, the ANSYS Fluent program also requires specifying the medium's porosity. In the model, a porosity of 0.9 was adopted.

In the model presented in the paper, the porous zone encompasses a selected area, vertically bounded by the riverbed surface ("wall_porous") and the upper surface of the computational domain ("open_porous"). This means that the PMM will be active throughout the height of this zone, both in the water and in the air. Since, in the VoF model, coefficients k and β are introduced separately for both phases, the model can be configured to introduce resistance only in water or both in water and air. The first case can simulate the presence of vegetation only below the water surface, while the second case can represent tall vegetation, such as reeds, limiting not only water movements but also airflow above its surface. The model applied the first variant, and no flow resistances were defined for the air. It's worth noting that the porous zone doesn't have to extend vertically throughout the entire computational domain. It can be located at the bottom, at the mean water level, or up to a specified height above the water surface. The last option allows for the consideration of vegetation of any height without disrupting the airflow above this zone.

Since the use of the SM requires the activation of the energy equation and consideration of thermal effects, the simulation model must specify the material parameters of the porous medium skeleton, such as density, specific heat, and thermal conductivity. This aspect is as problematic as determining the parameters k and β . In general, it is challenging to define the material because, in reality, plant zones can be highly diverse in terms of plant species, their proportions, and spatial distribution. Since

the author could not find relevant information, the simulation adopted material parameters corresponding to beechwood (Hrčka & Babiak, 2017). Density, specific heat, and thermal conductivity were set to 703.9 [kg/m³], 1900 [J/(kg·K)], and 0.23 [W/(m·K)], respectively. This estimation method is highly imperfect but safeguards against providing values in unrealistic ranges.

The study introduced a single porous zone; however, in a specific case study, it may be necessary to create multiple such zones to represent the different locations of various vegetation areas, or alternatively, a single zone with parameter variations in different parts, such as near the bottom or the surface. The author's previous experience indicates that the computational costs associated with porous zones are minimal, but dividing the domain into zones appropriately and generating a numerical mesh of sufficient quality may pose some challenges.

3.3. Configuration of Boundary Conditions

The boundary conditions were specified according to the requirements of the VoF model in the Open Channel version. For inlets, so-called velocity or mass inlets can be used. The difference is that the velocity specified at the velocity inlet applies to both phases (water and air) in the case of a velocity inlet, while the mass flow is provided only for the liquid phase, and the gas phase remains at rest. The ANSYS Fluent software documentation (ANSYS Fluent Theory Guide, 2022) mentions that mass inlets allow for greater computational stability, which can be significant for large and complex simulation models. In additional simulations (not shown in the article), it was verified that in the discussed example, the calculations are stable and correct even when all inlets are velocity inlets. Ultimately, it was decided that "inlet_big" and "inlet_duct" would be mass inlets, while "inlet_small", which is always below the liquid level, would be a velocity inlet. It was also assumed that only clean water flows through "inlet_big", and only dirty water with a slightly higher temperature and a slightly higher water level is introduced through "inlet_duct". Detailed information about the parameters at the inlets and outlets is presented in Tables 1 and 2. In the case of the outlet, parameter values (except pressure) are significant only when there is a backflow.

The symbols visible in tables denote respectively: T – temperature, ρ – density, μ – dynamic viscosity, A – cross-section area of the water stream, P – wetted perimeter, d_h – hydraulic diameter, v_n – velocity (normal to boundary), Re – Reynolds, number, \dot{m} – mass flow rate [kg/s], α_{dirty}^m – mass fraction of water-dirty, α_{dirty}^V – volume fraction of phase 2 in VoF, y_{bottom} – bottom level, y_{fs} – free surface level, l – characteristic length, $I_{\%}$ – turbulence intensity, k – turbulent kinetic energy, ω – specific dissipation rate. In the case of the outlet, parameter values (except pressure) are significant only when there is a backflow (denoted by index b).

As mentioned earlier, the simulation utilized the VoF model designed for Open Channel flow modeling. This option needs to be activated at each inlet or outlet that is not entirely filled with fluid and has a free surface. In the

Table 1 Boundary conditions at the inlets

	inlet_big	inlet_duct	inlet_small
type	mass-flow-inlet	mass-flow-inlet	velocity-inlet
T	283 [K]	288 [K]	283 [K]
ρ	999.7 [kg/m ³]	999.1 [kg/m ³]	999.7 [kg/m ³]
μ	0.001306 [Pa·s]	0.0011375 [Pa·s]	0.001306 [Pa·s]
A	5.7804 [m ²]	1.7846 [m ²]	0.196 [m ²]
P	7.8952 [m]	4.2597 [m]	-
d_h	2.9286 [m]	1.6758 [m]	0.25 [m]
v_n	1 [m/s]	1 [m/s]	0.5 [m/s]
Re	2241719 [-]	1471918 [-]	95683 [-]
\dot{m}_{mix}	5778.67 [kg/s]	1783.0 [kg/s]	98.15 [kg/s]
α_{dirty}^m	0	1	0
α_{dirty}^v	-	-	1
open channel	yes	yes	no
y_{bottom}	0 [m]	0 [m]	-
y_{fs}	0.9 [m]	1.0 [m]	-
inlet group ID	1	2	-
l	0.204999 [m]	0.117307 [m]	0.0175 [m]
$I_{\%}$	0.025722 [%]	0.027110 [%]	0.038152 [%]
k	0.000992 [m ² /s ²]	0.001102 [m ² /s ²]	0.000546 [m ² /s ²]
ω	0.280563 [1/s]	0.516768 [1/s]	2.437431 [1/s]

Table 2 Boundary conditions at the outlets

	outlet	open_river	open_porous
type	pressure-outlet		
T_b	283 [K]		
p	-	0 [Pa]	0 [Pa]
open channel	yes	no	no
y_{bottom}	0	-	-
y_{fs}	0.9 [m]	-	-
Outlet group ID	1	-	-
$\alpha_{dirty,b}^m$	0	0	0
$\alpha_{dirty,b}^v$	-	0	0
backflow pressure	total pressure	-	-
k_b	0.000992 [m ² /s ²]		
ω_b	0.280563 [1/s]		

simulation, these surfaces are “inlet_big”, “inlet_duct”, and “outlet”. The Open Channel variant requires defining the reference level (bottom level) and the position of the free surface of the fluid (free surface level). The necessity of providing these parameters gives some indications regarding the preparation of geometry and its placement in the global coordinate system. In the model, it was assumed that the bottom of the watercourse is flat and located at a height of $y = 0$. In the general case where the riverbed has a variable height, it would be advisable to set the zero level at the point of greatest depth. Another sensible assumption could be to position the domain so that the zero height corresponds to the water surface level. An important parameter in the ANSYS Fluent model is the inlet/outlet group ID. In the described model, the inlet “inlet_duct” had its default ID changed from 1 to 2. This modification enabled the definition of independent boundary conditions not linked to the “inlet_big”, which by default also had ID = 1.

Another aspect of defining conditions at inlets and outlets is specifying parameters related to turbulence modeling. The Reynolds number indicates that the flow is turbulent, and therefore, this aspect must be taken into account. Due to the lack of other assumptions, the universal $k - \omega$ SST model was chosen, providing good results in both the boundary layer and the depth of the flow. The following formulas ([Ansys Fluent User's Guide, 2022](#)) were used to estimate the boundary values of turbulence parameters:

$$k = \frac{3}{2} (v_{inlet} \cdot I_{\%})^2, \tag{5}$$

$$\omega = \frac{k^{0.5}}{0.09^{0.25} \cdot l}, \tag{6}$$

where $l = 0.07 \cdot d_h$ and $I_{\%} = 0.16 \cdot \text{Re}_{d_h}^{-\frac{1}{8}}$.

Equations (5)-(6) were used to estimate the values of k and ω at all three inlets, taking into account the geometry, the assumed free surface level, and the specified

velocities in the simulation. At the outlets, the values of these parameters were not computed; instead, they were assumed to be the same as those prevailing at the largest inlet. It is worth emphasizing that at the outlets, the values of k and ω have some significance only when there is a possibility of reverse flow.

In addition to the inlets and outlets, the model includes walls. It was assumed in the model that these walls are adiabatic, but one can imagine situations in which the water temperature would change, affecting the temperature of the ground. In such cases, it would be necessary to specify heat fluxes on individual walls and appropriate material parameters. It turned out that there is relevant literature, and the issue of material properties is not as problematic as described during the configuration of the porous zone.

In the simulation model, it was assumed that the bridge supports (“wall_bridge”) are made of concrete. Sample concrete parameters were taken from the work (Jaskulski, et al. 2019) (mixture C-A): density equal to 2529 [kg/m³], specific heat equal to 765 [J/(kg·K)], thermal conductivity equal to 2.23 [W/(m·K)]. It was assumed in the model that the material assigned to the other walls limiting the movement of water, i.e., “wall_river”, “wall_porous” and “wall_stones” is sand. Material parameters were determined based on the paper (Hamdhan & Clarke, 2010), assuming saturated coarse sand: density equal to 2080 [kg/m³], specific heat equal to 1483 [J/(kg·K)], thermal conductivity equal to 3.72 [W/(m·K)]. One can discuss whether the materials and their parameters were adopted correctly; this comment also applies to the previously described parameters of water vegetation. However, it should be emphasized that, in general, the values are within realistic ranges, and the details will depend on the specific case, most often related to some actually existing watercourse.

3. 4. Preparing the numerical simulation

One of the elements of configuring the simulation model is specifying details regarding the solution methodology. Following recommendations from the documentation of the used software, the following options were set: “Pressure-Velocity Coupling” – “Coupled”; “Transient Formulation” – “Bounded Second Order Implicit”; “Spatial Discretization for Pressure” – “PRESTO!”; “Spatial Discretization for Volume Fraction” – “Compressive”. The ANSYS Fluent program provides a tool to check the correctness of the VoF model during the initialization stage. Upon pressing the “VoF Check” button in the calculation initialization section, two additional suggestions appeared in the program terminal regarding enabling the options “Warped-Face Gradient Correction” and “High Order Term Relaxation”. Other settings were left unchanged, including relaxation parameter values and convergence criterion values.

To monitor the progress of the water mixing process, a visualization was prepared, automatically saved at each time step. Monitors were defined for the force acting on the bridge supports and the total mass of dirty water in the flow. The calculations were initialized using a hybrid method and ran for 6000 iterations with a time step of 0.01

[s]. These settings allowed modeling a 60-second process. The calculations were performed in double precision using 16 computational cores, which was limited by the available license. The parameters of the computer used were as follows: AMD Epyc 7662 processor, 64 cores, 64-bit architecture, 256 MB L3 cache, 128 GB RAM, 3200 MHz RAM clock speed, DDR memory type. The actual simulation time was 288 hours. Although the ANSYS Fluent package offers specialized modules for variant analysis, sensitivity analysis, and optimization based on selected criteria (e.g., tools like Direct Optimization, Parameter Correlations, or Response Surface), I chose not to perform these studies. Given the extended simulation time, the effect of various model parameters and settings on computation time was not evaluated. It was only observed that increasing the time step to 0.1 [s] resulted in increased residuals and interrupted calculations.

3.5. Results of Calculations

In Figures 5-8, the system's state is visible at selected time steps. The legend on the left side of the figures refers to the mass fraction of dirty water, represented by two transparent iso-surfaces defined for a dirty water fraction equal to 0.5 and 0.25 (these cannot be distinguished in the presented figures). This visualization method means that dirty water actually occupies a slightly larger space, but its fraction there is lower than 25%. The legend at the bottom refers to the water velocity and is overlaid on an iso-surface representing the water surface level.

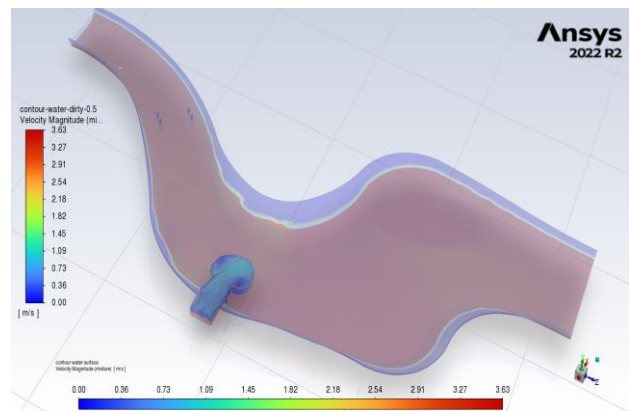


Fig. 5 Visualisation of the flow at t = 0 [s]

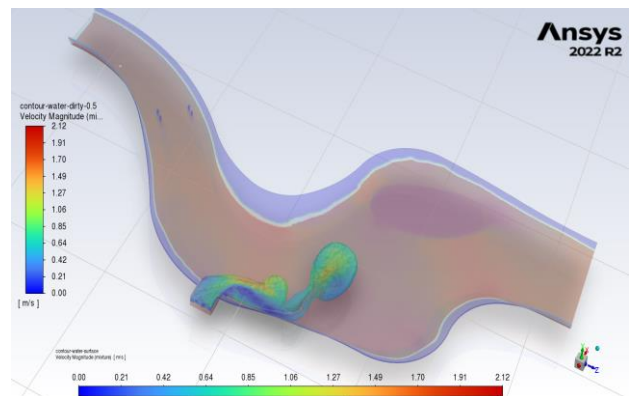


Fig. 6 Visualisation of the flow at t = 15 [s]

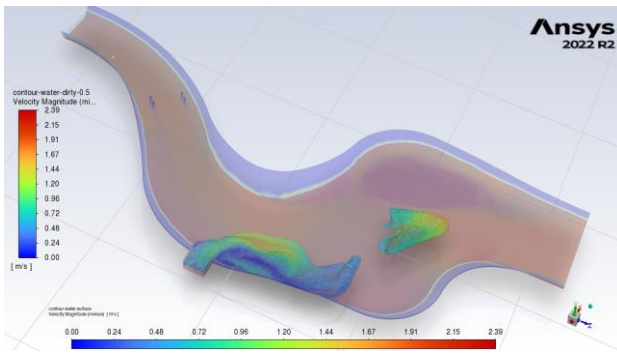


Fig. 7 Visualisation of the flow at $t = 30$ [s]

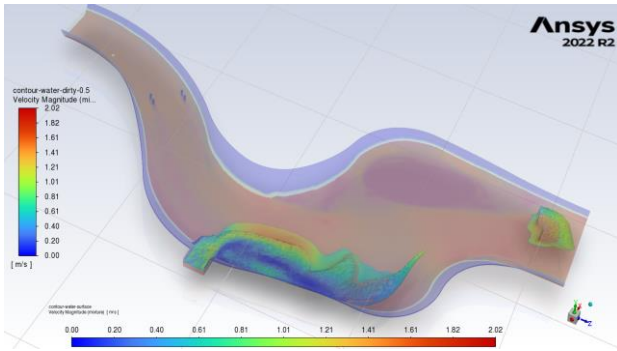


Fig. 8 Visualisation of the flow at $t = 60$ [s]

Observing the edges of the watercourse, it can be noticed that, after initiating the simulation, a small wave moves along the water surface. This is a singular phenomenon that occurs at the beginning of the simulation and does not hold significant importance in the context of the research. It can also be seen that the flow significantly slows down in the area of the porous zone. A slight slowdown is also visible behind the bridge supports. The system's behavior is generally in line with expectations, and there are no noticeable effects suggesting incorrect parameter settings. In the study, it was considered that a simulation time of 60 [s] allows determining whether the developed model works correctly, and there is no need for further simulations. Practically significant is the established relationship between simulation time and computational time. In the described example, modeling 1 second of flow takes about 4.8 hours of real-time. These times will, of course, be different on another computer, but they allow estimating the capabilities and the realistic time scale of modeling a specific flow. It can be assumed that there are more optimal settings for the simulation model, allowing for faster results, but very large differences in this area, on the order of several hundred or even tens of percent, are not to be expected.

The conducted tests showed that the simulation duration increases proportionally to the assigned computation time. With data for both times for a given computational machine, it is possible to easily estimate the simulation duration for another, selected computational period, which allows for assessing whether such waiting time is acceptable. Computational performance can be improved by using parallel processing. Performance tests of ANSYS Fluent published in the literature show that

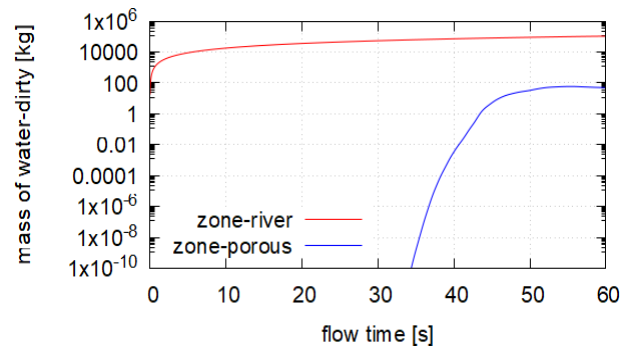


Fig. 9 Changes in the mass of dirty water in the river zone and in the vegetation zone over time

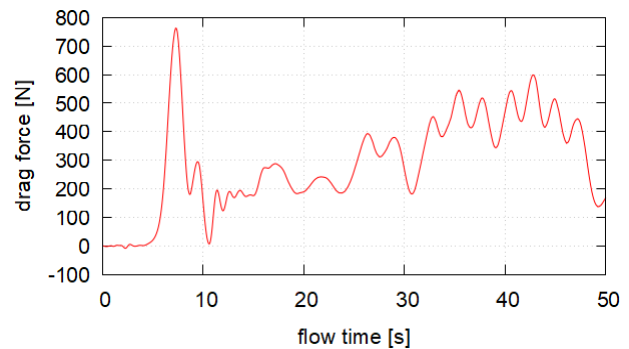


Fig. 10 Changes over time in the resultant force acting on the bridge supports

computational acceleration through parallel data processing is effective until the communication time between processors starts to dominate. A key factor in this process is access to appropriate computational machines and licenses.

In Fig. 9, the record of the dirty water mass monitor with a division into zones is visible. It can be observed that dirty water practically does not penetrate the porous zone. This is due to the location of this zone, somewhat on the sidelines of the main flow, and the low water velocity inside it. This effect indicates that considering the existence of aquatic vegetation zones can be crucial in modeling the propagation of pollutants in watercourses. It can also be inferred that pollutants that enter the vegetation zone may linger there for a relatively long time, forming local deposits.

In Fig. 10, changes in the resultant force acting on the four supports defined in the model are visible. It can be seen that the force value changes over time, confirming the non-stationary nature of the flow. Of course, force monitors (or force moments) can be defined for each support separately. It seems that in environmental analyses, the aspect of hydrodynamic interactions may not be of great importance, although the mere presence of various barriers or objects in the riverbed will affect the flow field, and thus also the spatial distribution of individual mixture components. Since the supports are located upstream from the point of supplying dirty water, one could consider removing this element from the model. This would reduce the grid size and slightly shorten the calculation time. Nevertheless, such a step could only be

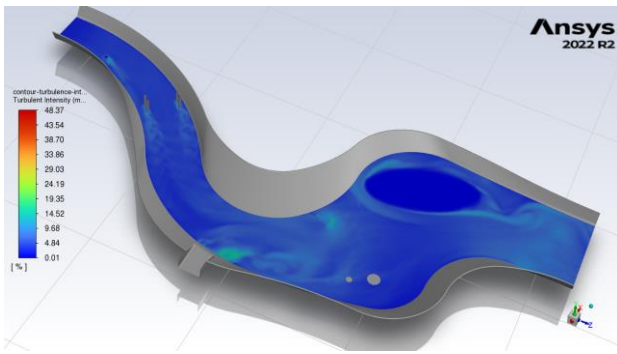


Fig. 11 Distribution of turbulence intensity at a height of 0.05 [m] above the riverbed at $t = 60$ [s]

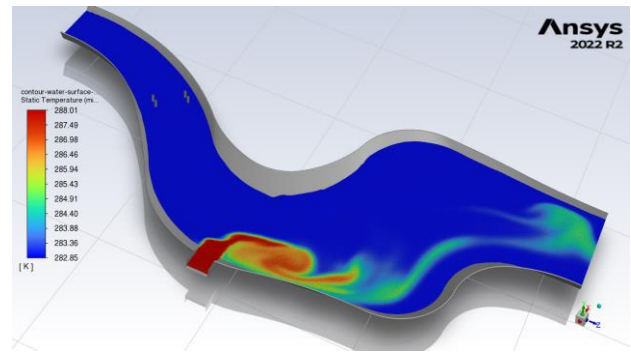


Fig. 13 Temperature distribution at the free surface of water at $t = 60$ [s]

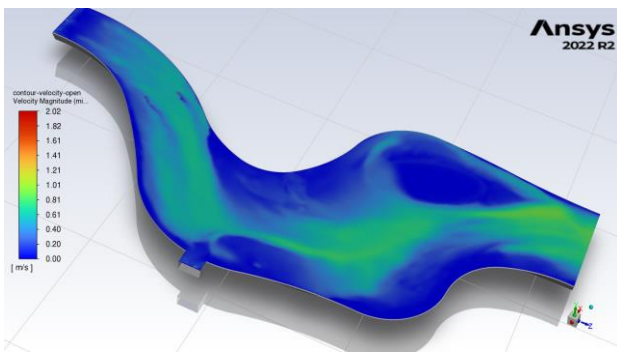


Fig. 12 Velocity distribution on the upper surface of the computational domain at $t = 60$ [s]

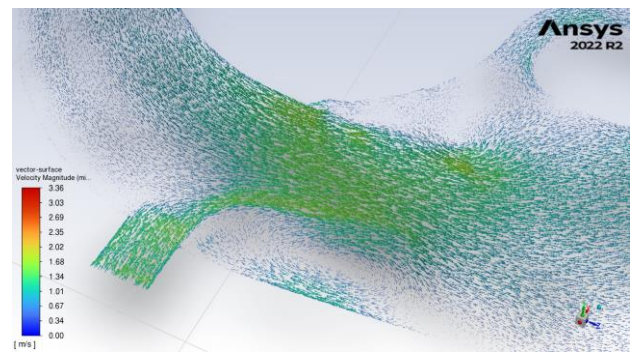


Fig. 14 Visualization of selected recirculation areas for $t = 60$ [s]

taken under the assumption that the effect of the supports' interaction will not be significant in the analysis of the propagation of solid particles, as discussed further.

The effect of the presence of obstacles on the bottom (“wall_stones”) is not strongly noticeable. Nevertheless, downstream of the obstacle, a small band of increased turbulence intensity appears (Fig. 11), indicating that the mixing process of the water streams is accelerated in this area. Perhaps the interruption of the dirty water stream, visible in Fig. 7, is initiated or enhanced by the presence of obstacles on the bottom in this location. The open question is whether such interactions will be important for the overall analysis of pollutant propagation or not. If not, removing these types of elements would once again allow for a reduction in the size of the computational grid and a shortening of the simulation time.

In the numerical model, no parameters defining the air velocity above the water surface have been specified. Due to the boundary conditions set at the inlets, the air velocity in the “inlet_big” and “inlet_duct” planes is initially zero. However, due to viscosity effects, the air begins to move, reaching velocities of up to 2 [m/s] in certain areas. Where the water velocity is low, particularly in the porous zone, air movement is also limited. Figure 12 illustrates the described phenomenon, showing the velocity distribution on the surfaces of “open_river” and “open_porous”.

In the simulation model, it was assumed that the temperature of pollutants is higher than the water temperature in the river. In Fig. 13, the range of thermal

influence of pollutants and changes in temperature values in individual regions can be observed. According to the basic principles of thermodynamics, the thermal aspect will depend on the amount of introduced pollutants, the specific heat of the contaminating phase, and the temperature difference in the system. Details will depend on the specific configuration; however, it is evident that the impact of wastewater, in a broad sense, can be significant not only by introducing pollutants into the environment but also by causing temperature changes, which, in turn, will affect the local conditions of the biosystem.

The flow analysis can be complemented by recirculation zones, which are well visible in visualizations depicting the vector field of velocity. Generally, recirculation zones can be expected in water streams, but numerical simulations are necessary to precisely determine their location, extent, and intensities. In the analyzed flow, several recirculation zones are present, with the largest ones located directly behind the channel bringing in pollutants and at the opposite side, behind the bend in the riverbank (Fig. 14).

In the flow, Karman vortices can be observed appearing behind the bridge supports (not shown here). This phenomenon is consistent with expectations, although the detailed path of the Karman vortices is not very well-defined due to the relatively sparse grid used for this spatial scale. The numerical grid can, of course, be refined around and behind the bridge supports (or generally on small features), but the question remains

whether it is necessary in this analysis. When modeling the behavior of watercourses, one should avoid such refinements, accepting the loss of detail in favor of scale.

3.6 Configuration of the Discrete Phase Model

In the tests, it was assumed that the ability to model any particulate matter in the form of a particle cloud would be examined. To achieve this goal, the aforementioned Discrete Phase Model was used, excluding the influence of particles on the liquid phase. The application of this model requires performing main calculations, defining injections, and conducting visualizations. Since the velocity field is known at this stage, particle trajectories are calculated based on this field and the forces acting on the particle. The primary factors influencing particle motion are the force due to gravity, calculated based on the material properties and particle diameter, and the drag force, which arises from the surrounding mass of the moving fluid. The test utilized the simplest possible variant of the model, without delving into numerous details that are difficult or even impossible to determine at this stage of the research. In the example, the “inlet_small” plane was chosen as the injection area, and the material for the particles was selected from the default materials available in the software database, named “ash-solid”. On the walls, the reflection type boundary condition was applied. The details of the DPM model configuration are presented in Tab. 3. Particle trajectories, colored according to the time spent in the computational domain, are visible in Fig. 15.

Figure 16 presents the results of the DPM acting when massless particle were used. It can be observed that some particles enter one of the recirculation zones and turn upstream, ultimately extending their residence time in the domain. The figure also shows that the main stream is, for a certain stretch, separated from the flow incoming from the side inlet, as particles do not penetrate into it. This occurs only in the downstream region, where the mixing processes of both streams are advanced.

A practical issue should be noted. The results so far were based on the transient model (Transient). To apply the DPM model in the one-way variant, the analysis must be switched to steady-state (Steady). Without this, visualization cannot be performed, even with correct source and injection settings, and the program offers no explanation for this issue.

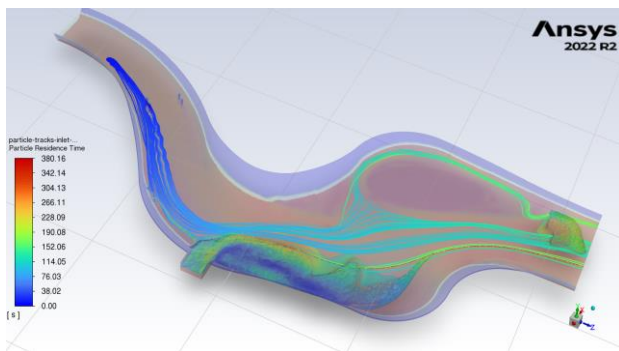


Fig. 15 Particle trajectories of the solid phase “ash-solid” at t = 60 [s]

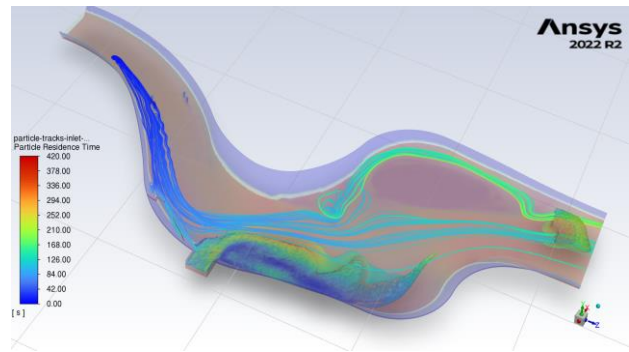


Fig. 16 Particle trajectories of the solid phase “massless” at t = 60 [s]

During the investigations, several additional tests were conducted, considering what could potentially be useful in the analysis of pollutant propagation in watercourses. It was confirmed that the Named Expression tool allows for dynamic changes in velocity and liquid level over time. An example instruction describing the variation of velocity over time has the following form:

$$IF(t < 1[s], 1[m/s], 1.01[m/s] - 0.01 * 1[m/(s*s)] * t)$$

The change in water level can be described, for example, by the following expression:

$$0.9[m] * (1[s] - 0.002 * t) / 1[s]$$

In more complex situations, such as when it is necessary to define the velocity distribution at the inlet or when the function describing changes over time is particularly intricate, the User Defined Functions mechanism can be applied to describe these changes. This mechanism requires creating code fragments in the C language, which replace default solutions. Details regarding the creation of such functions are described in the documentation ([Ansys Fluent Customization Manual, 2022](#)).

3.7. Practical Applications of the Model in Crisis Situations

The primary obstacle in using three-dimensional pollution propagation models is the currently limited computational power, which is insufficient for the needs of full-scale simulations. The presented model utilizes restricted spatial and temporal domains, making it most applicable in emergency situations, such as sudden accidents. Unfortunately, both model preparation and computation are still too time-consuming to enable the development of real-time rescue scenarios based on full 3D simulations. However, the one-way DPM model, which relies on a precomputed velocity field, offers certain possibilities. A potential solution could involve preparing models and simulations in advance for sensitive areas and several typical conditions, such as different seasons. After a specific incident occurs, the DPM analysis could be quickly performed by defining only the emission source and the parameters of particles representing the given substance (these data can also be prepared beforehand). For example, in cases where a watercourse intersects with or is adjacent to a pipeline or

Table 3 Settings of the DPM model applied in the simulation

Parameter	Setting
Injection type	surface
Injection surfaces	inlet_small
Particle type	inert
Material	ash-solid
Diameter distribution	uniform
Inject using face normal direction	on
Diameter	0.0001 [m]
Temperature	283 [K]
Velocity magnitude	0.5 [m/s]
Total flow rate	1.0 [kg/s]

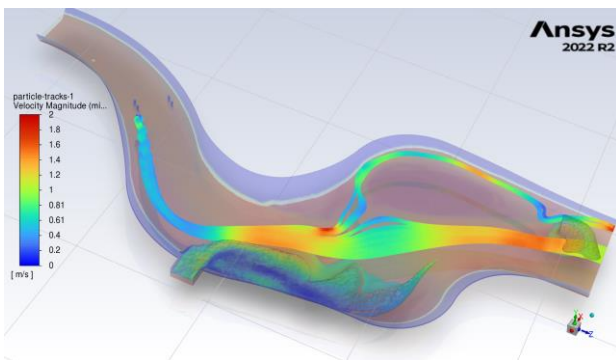


Fig. 17 An example of particle injection at an arbitrary defined spherical region in the computational domain at $t = 60$ [s]

a tank containing oil, sewage, or another hazardous fluid, and there is a risk of leakage, a simulation could be conducted swiftly. Upon detecting such an event, it would suffice to define the location and parameters of the emission source, and the simulation results could promptly provide essential information about the potential spread of pollution.

In the original model, it was assumed that the location of the injection source was fixed. However, ANSYS Fluent provides the flexibility to define this source later in the process. To achieve this, you can use the mesh region definition tool (Region Register). This tool allows the creation of regions in the shape of a cuboid, sphere, or cylinder. It is crucial to enable the "Create Volume Surface" option during the region generation, as the surface of the defined region will serve as the injection surface, just as it did with the "inlet_small" surface in the original setup. The remaining steps for defining the DPM model remain unchanged from the previous configuration.

In Fig. 17, the effect of using a spherical injection point is shown, positioned at coordinates 10.0, 0.2 and 20.0 [m] with a diameter of 0.3 [m]. The calculations were performed using the same data as presented in Table 2.

Numerical simulations of selected systems can be cataloged and used as templates, significantly reducing response time by eliminating the need for real-time simulation setup. This process could be further streamlined when integrated with real-time pollution monitoring systems. These systems would not only detect

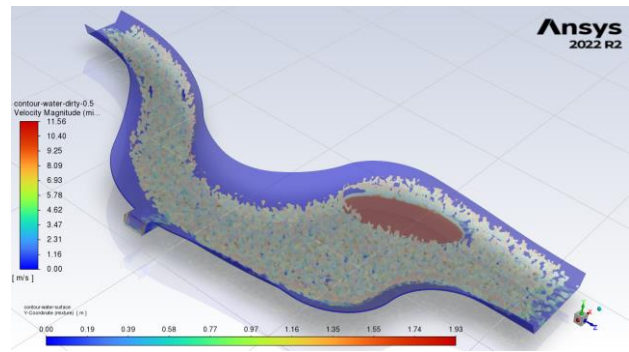


Fig. 18 The effect of incorrectly assuming the density of the mixture

contamination, identify its location, and assess its intensity but could also generate files with user-defined functions (UDFs) to describe the source and injection parameters (a capability supported by ANSYS Fluent). The simulation workflow would then be simplified to loading the appropriate template into Fluent, compiling the UDFs, and producing the visualization.

3.8. Errors and Issues in Model Configuration

During the model creation, several errors and challenges arose, prompting the need to highlight them for readers.

The primary issue was the absence of dirty water in the flow. Despite multiple checks and the creation of a simpler flow model with similar settings that worked correctly, the problem persisted until the server was restarted and ANSYS Fluent relaunched. Upon reviewing the boundary conditions, it was found that the labels for the mass fractions of clear and dirty water were incorrect, leading to confusion about the components. Although the cause of the error was unclear, it was likely due to the program referencing the wrong component. The issue was resolved by resetting the program settings. Users are advised to utilize options for saving or loading model configurations and comparing current settings with default ones.

The second issue stemmed from the author's misunderstanding of a detail in configuring the Species model. Following ANSYS instructions, it was assumed that defining the material properties for "water-clear" and "water-dirty" completed the mixture definition. However, the default material in ANSYS Fluent is air, which remains unchanged even when other materials are used. This misconfiguration led to a simulation where the water level decreased over time and the surface became irregular, resembling evaporation from the riverbed (Fig. 18). Initial troubleshooting focused on boundary conditions and inlet types without success. Ultimately, it was stated that the mixture density was still set to air's default value, explaining the model's behavior. Changing the density option to "volume-weighted-mixing-law" in the mixture definition panel resolved the issue.

During attempts to resolve the previous issue, the author mistakenly defined the "wall-river" surface, omitting a small fragment at the edge of the porous zone,

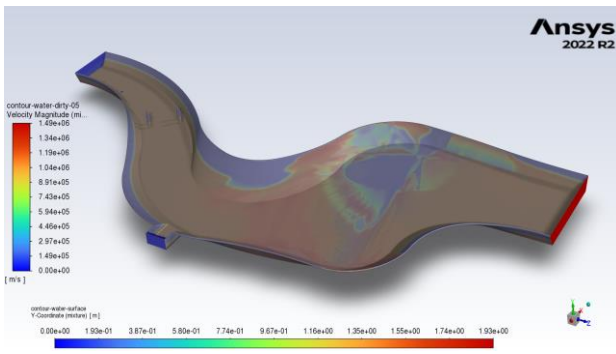


Fig. 19 Effect of generating a grid with too low quality

which created a gap in the boundary layer. Although the grid quality indicators were still acceptable, the model's behavior (degradation of the solution and computation interruption) pointed to a local grid problem (Fig. 19). The error was quickly identified because the sum of surfaces with specific wall names had not been checked against the total number of defined surfaces in the model. This experience highlights the importance of careful organization and naming of surfaces in complex geometries, such as those derived from water body depth maps. It is recommended to verify the number of named surfaces against the total count to avoid issues during grid generation and boundary condition definition. In this case, there were 72 total walls, including two connecting the river and vegetation zones. After entering the ANSYS Fluent module, it is good practice to review the names and types of all boundaries in the "Boundary conditions" section to ensure they match expectations; any discrepancies should prompt a return to the geometry or grid generation stages. Undefined surfaces in ANSYS Fluent are interpreted as walls, with names consisting of "wall" followed by a number.

During one attempt, unusual flow behavior was observed because the surface for standard data initialization was not specified, causing incorrect velocity vector directions at the main inlet. After correcting the initialization method, the results matched expectations. It was also confirmed that hybrid initialization is equally effective and was used in subsequent simulations.

For those experienced in using the models discussed, the highlighted issues may seem obvious. However, the vast field of Computational Fluid Dynamics (CFD) makes it impossible to master all methods and techniques at an expert level. Some challenges arise from the implementation of specific software rather than general theory, and not all potential errors in simulation model preparation can be outlined. This description aims to underline that creating a simulation model, particularly one beyond the previous experience, can be a lengthy and complex process. Configuring the model presented in the paper was particularly challenging, revealing issues sometimes after several days of calculations.

4. CONSLUSIONS

The conducted research allowed for the definition of the following observations and conclusions:

Successful integration of multi-physics models. The study confirms the feasibility of using a multi-physics approach in a single simulation setup, effectively combining the Volume of Fluid (Open Channel version), Species, Porous Media, and Discrete Phase Models. To ensure proper function, the Species Model must be defined prior to the Volume of Fluid model.

Guidelines for pollutant modeling strategies. When simulating pollutant dispersion in watercourses, using the Discrete Phase Model initially can be advantageous as it requires less computational power than the Species Model. In cases focusing on the near-bed zone, omitting the Volume of Fluid model can dramatically reduce computational demands, allowing for larger-scale spatial or temporal modeling.

Complexity and requirements of the Species Model. Applying the Species Model involves accounting for the energy equation, which requires the input of various material and situational parameters (such as specific heat, heat transfer coefficients, and boundary heat fluxes). These parameters often require precise measurement, calculation, or access to reliable data sources.

Simulation stability and flexibility. The model allows for various inlet types (velocity or mass) and initialization methods (standard or hybrid). Testing revealed that these configurations did not affect simulation stability, providing flexibility in model setup.

Estimation of model scale feasibility. The conducted simulations offer an initial understanding of the realistic spatial and temporal scales that are achievable on current computing hardware, giving insight into practical applications.

Challenges with the Porous Media Model. Integrating the Porous Media Model presented a significant challenge due to the complexity of accurately representing vegetation zones in water. Lack of precise permeability data and variability in vegetation characteristics mean that further studies, especially experimental ones, are crucial to developing a comprehensive parameter set. The findings indicate the potential value in creating a standardized approach for modeling water vegetation with multiple porous zones. An additional challenge may involve preparing geometry that includes vegetation zones with complex shapes or a collection of such zones.

Complexities in Discrete Phase Model configuration. Setting up the Discrete Phase Model (DPM) brought particular difficulties, especially regarding particle interactions with the riverbed. Current boundary conditions may be inadequate to capture these interactions, signaling a need for additional experimental and modeling efforts. Realistic particle behavior in simulations might require new phenomena or processes, representing an under-explored area of study.

Computation time and performance limitations. Extended computational times and slow responsiveness of the ANSYS modules highlight that large-scale 3D multiphysics models are still constrained by available

computational power. However, the study illustrates that meaningful insights can still be derived within current technical limitations, identifying knowledge gaps that future research can fill to extend modeling capabilities in spatial and temporal dimensions.

Potential model expansions with enhanced computing power. With increased computational resources, the model could be enhanced in several ways: a) Additional Injection Points: Introducing more sources of solid particles, such as above the water surface, could enable analysis of settling patterns and propagation inside the water; b) Modeling the Dynamic Riverbed: Using an Eulerian Multiphase Model in the fluid-solid variant (e.g. Gidaspow model), in tandem with DPM, would offer greater detail on particle deposition over time. c) Biochemical and Environmental Effects: Expanding chemical and biochemical aspects to explore pollutant degradation, potentially integrating dissolved gases. d) Cavitation and Impact Analysis: Adding cavitation effects for obstacles and objects on the riverbed could simulate erosion. e) Oil Spill Modeling: Extending the Volume of Fluid model to simulate oil pollutants' spread across water surfaces. f) Thermal Exchange Modeling: Adding a surrounding solid zone could allow analysis of heat exchange between water and the underlying ground.

The potential application of simulation models in emergency situations. The research demonstrated that it is possible to define injection sources in models based on full 3D simulation results, with the sources being located at arbitrary positions, and utilize the DPM model for rapid crisis situation analysis. The integration of the simulation model with real-time monitoring systems was also considered, through the use of user-defined functions (UDFs), which could potentially enable efficient and fast responses to incidents.

Identification of errors and issues in model configuration. This study highlights the importance of thorough verification of geometry details, boundary conditions and material properties, as even minor oversights can lead to significant discrepancies in model behavior. Continuous learning and attention to detail in the configuration process can enhance the reliability and quality of CFD simulations.

CONFLICT OF INTEREST

The author declares no conflicts of interest.

AUTHORS CONTRIBUTION

Sobieski W.: conceptualization, data curation, formal analysis, investigation, methodology, resources, software, supervision, validation, visualization, writing – original draft, writing – review & editing.

FUNDING

This study was funded by Polish Ministry of Science and Higher Education in the frames of the statutory research.

REFERENCES

- Agranat, V., Romanenko, S., & Perminov, V. (2021). Mathematical modelling of river pollution as a result of pipeline damage. *Chemical Engineering Transactions*, 88, 481-486. <https://doi.org/10.3303/CET2188080>
- Alvir, M., Grbčić, L., Sikirica, A., & Kranjčević, L. (2022). OpenFOAM-ROMS nested model for coastal flow and outfall assessment. *Ocean Engineering*, 264, 112535. <https://doi.org/10.1016/j.oceaneng.2022.112535>
- Arthur, J. K. (2018). Porous media flow transitioning into the forchheimer regime: a PIV study. *Journal of Applied Fluid Mechanics*, 11(2), 297-307. <https://doi.org/10.29252/jafm.11.02.28262>
- ANSYS Inc. (2022, January). *Ansys Fluent Theory Guide*, Release 2022R1.
- Bhatnagar, P., Gross, E., & Krook, M. (1954). A model for collision processes in gases: I. Small amplitude processes in charged and neutral one-component systems. *Physical Review*, 94, 511-525.
- Bondelind, M., Sokolova, E., Karlsson, D., & Björklund, K. A. (2020). Hydrodynamic modelling of traffic-related microplastics discharged with stormwater into the Göta River in Sweden. *Environmental Science and Pollution Research*, 19, 24218-24230. <https://doi.org/10.1007/s11356-020-08637-z>
- Chu, K., Wang, B., Xu, D., Chen, Y., & Yu, A. (2011). CFD-DEM simulation of the gas-solid flow in a cyclone separator. *Chemical Engineering Science*, 66, 834-847. <https://doi.org/10.1016/j.ces.2010.11.026>
- Cundall, P., & Strack, O. (1979). A discrete element model for granular assemblies. *Géotechnique*, 29, 47-65.
- Diener, E. (2019). *Modelling the circulation and spread of pollution in lake Rådasjön under conditions of climate change* [Master's thesis, Chalmers University of Technology].
- Hadžiabdić, M., Hafizović, M., Ničeno, B., & Hanjalić, K. (2022). A rational hybrid RANS-LES model for CFD predictions of microclimate and environmental quality in real urban structures. *Building and Environment*, 217, 109042. <https://doi.org/10.1016/j.buildenv.2022.109042>
- Hamdhan, I., & Clarke, B. (2010). *Determination of thermal conductivity of coarse and fine sand soils*. Proceedings of the World Geothermal Congress 2010 (pp. 1-7).
- Hrčka, R., & Babiak, M. (2017). *Wood thermal properties*. Wood in Civil Engineering. IntechOpen. <https://doi.org/10.5772/65805>
- Jaskulski, R., Glinicki, A., Kubissa, W., & Dabrowski, M. (2019). Application of a non-stationary method in determination of the thermal properties of radiation

- shielding concrete with heavy and hydrous aggregate. *International Journal of Heat and Mass Transfer*, 130, 882-892. <https://doi.org/10.1016/j.ijheatmasstransfer.2018.07.050>
- Korotenko, K., Mamedov, R., Kontar, A., & Korotenko, L. (2004). Particle tracking method in the approach for prediction of oil slick transport in the sea: Modelling oil pollution resulting from river input. *Journal of Marine Systems*, 48, 159-170. <https://doi.org/10.1016/j.jmarsys.2003.11.023>
- Lee, I. B., Bitog, J., Seo, H. S. W., Seo, I. H., Kwon, K. S., Bartzanas, T., & Kacira, M. (2013). The past, present and future of CFD for agro-environmental applications. *Computers and Electronics in Agriculture*, 93, 168-183. <https://doi.org/10.1016/j.compag.2012.09.006>
- Li, J., Guo, F., & Chen, H. (2024). A study on urban block design strategies for improving pedestrian-level wind conditions: CFD-based optimization and generative adversarial networks. *Energy & Buildings*, 304, 113863. <https://doi.org/10.1016/j.enbuild.2023.113863>
- Liu, G., & Liu, M. (2003). *Smoothed particle hydrodynamics*. World Scientific Publishing. <https://doi.org/10.1142/5340>
- Ma, G., Li, T., Wang, Y., & Chen, Y. (2019). Numerical simulations of nuclide migration in highly fractured rock masses by the unified pipe-network method. *Computers and Geotechnics*, 111, 261-276. <https://doi.org/10.1016/j.compgeo.2019.03.024>
- Montazeri, A., Chahkandi, B., Gheibi, M., Eftekhari, M., Waclawek, S., Behzadian, K., & Campos, L. (2023). A novel AI-based approach for modelling the fate, transportation and prediction of chromium in rivers and agricultural crops: A case study in Iran. *Ecotoxicology and Environmental Safety*, 263, 115269. <https://doi.org/10.1016/j.ecoenv.2023.115269>
- Omni Calculator. (2023, December 1). *Water viscosity*. Retrieved from <https://www.omnicalculator.com/physics/water-viscosity>
- Poursaeid, M. (2023). An optimized extreme learning machine by evolutionary computation for river flow prediction and simulation of water pollution in Colorado River Basin, USA. *Expert Systems with Applications*, 233, 120998. <https://doi.org/10.1016/j.eswa.2023.120998>
- Sobieski, W. (2011). The basic equations of fluid mechanics in form characteristic of the finite volume method. *Technical Sciences*, 14(2), 299-313.
- Sobieski, W. (2013). The basic closures of fluid mechanics in form characteristic for the finite volume method. *Technical Sciences*, 16(2), 93-107.
- Sobieski, W., & Šarler, B. (2023). Numerical methods in fluid mechanics – An overview. *Technical Sciences*, 26, 185-218.
- Sobieski, W., Lipinski, S., Dudda, W., Trykozko, A., Marek, M., Wiacek, J., Matyka, M., & Golembiewski, J. (2016). *Granular porous media* (in Polish). Department of Mechanics and Fundamentals of Machine Design, Olsztyn.
- Sukop, M., & Thorne, D. (2006). *Lattice boltzmann modeling – an introduction for geoscientists and engineers*. Springer. <https://doi.org/10.1007/978-3-540-27982-2>
- Veli, S., Arslan, A., Isgoren, M., Bingol, D., & Demira, D. (2021). Experimental design approach to COD and color removal of landfill leachate by the electrooxidation process. *Environmental Challenges*, 5, 100369. <https://doi.org/10.1016/j.envc.2021.100369>
- Zaidi, A. A. (2020). Resistance force on a spherical intruder in fluidized bed. *Journal of Applied Fluid Mechanics*, 13(4), 1027-1035. <https://doi.org/10.29252/jafm.13.03.30626>
- Zheng, X. G., Pu, J. H., Chen, R. D., Liu, X. N., & Shao, S. D. (2016). A Novel explicit-implicit coupled solution method of swe for long-term river meandering process induced by Dambreak. *Journal of Applied Fluid Mechanics*, 9(6), 2647-2660. <https://doi.org/10.29252/jafm.09.06.25969>
- Zieminska-Stolarska, A., & Skrzypski, J. (2012). Review of mathematical models of water quality. *Ecological Chemistry and Engineering*, 19(2). <https://doi.org/10.2478/v10216-011-0015-x>
- Zima, P. (2019). Simulation of the impact of pollution discharged by surface waters from agricultural areas on the water quality of Puck Bay, Baltic Sea. *Euro-Mediterranean Journal for Environmental Integration*, 4(16). <https://doi.org/10.1007/s41207-019-0104-2>
- Xue, J., Yuan, C., Ji, X., & Zhang, M. (2024). Predictive modeling of nitrogen and phosphorus concentrations in rivers using a machine learning framework: A case study in an urban-rural transitional area in Wenzhou, China. *Science of the Total Environment*, 910, 168521. <https://doi.org/10.1016/j.scitotenv.2023.168521>